RESEARCH ARTICLE

Differential expression of islet glutaredoxin 1 and 5 with high reactive oxygen species production in a mouse model of diabesity

Sebastian Friedrich Petry[1]*, Fatemeh Sharifpanah[2], Heinrich Sauer[2], Thomas Linn[1]

1 Clinical Research Unit, Center of Internal Medicine, Justus Liebig University, Giessen, Germany,
2 Department of Physiology, Faculty of Medicine, Justus Liebig University, Giessen, Germany

* sebastian.petry@innere.med.uni-giessen.de

Abstract

The onset and progression of diabetes mellitus type 2 is highly contingent on the amount of functional beta-cell mass. An underlying cause of beta-cell decay in diabetes is oxidative stress, which markedly affects the insulin producing pancreatic cells due to their poor antioxidant defence capacity. Consequently, disturbances of cellular redox signaling have been implicated to play a major role in beta-cell loss in diabetes mellitus type 2. There is evidence suggesting that the glutaredoxin (Grx) system exerts a protective role for pancreatic islets, but the exact mechanisms have not yet been elucidated. In this study, a mouse model for diabetes mellitus type 2 was used to gain further insight into the significance of Grx for the islets of Langerhans in the diabetic metabolism. We have observed distinct differences in the expression levels of Grx in pancreatic islets between obese, diabetic db mice and lean, non-diabetic controls. This finding is the first report about a decrease of Grx expression levels in pancreatic islets of diabetic mice which was accompanied by declining insulin secretion, increase of reactive oxygen species (ROS) production level, and cell cycle alterations. These data demonstrate the essential role of the Grx system for the beta-cell during metabolic stress which may provide a new target for diabetes mellitus type 2 treatment.

Introduction

Diabetes mellitus type 2 is hallmarked by a progressive loss of functional beta-cell mass. As from the early prediabetic stages of the disease onwards, the Islets of Langerhans suffer the detrimental effects of hyperglycaemia, free fatty acids, and inflammation [1]. As stress levels exceed the beta-cell's coping capacity, insulin secretion fades [2, 3]. Furthermore, oxidative stress and impaired redox signaling play a pivotal role in beta-cell decay [4]. The redox regulation of cellular processes ensures cell viability and function [5]. A major actor in redox signaling and maintenance of redox balance is the glutaredoxin (Grx) system. It consists of NAPDH, glutathione, glutathione reductase and the oxidoreductase glutaredoxin. Its influence on cellular processes is based on reversible post-translational de-glutathionylation of their target's cysteine residues. In mammals, there are four glutaredoxins, characterized as mono- or dithiol

Grx depending on the number of redox-active cysteine-residuals in their active center. The dithiol Grx1 was originally found to reduce ribonucleotides and thus to ensure DNA synthesis in E. coli [6, 7]. It is mainly located in the cytoplasm, but was also reported in the intermembrane space of mitochondria and the nucleus [8, 9]. It is a major actor in the thiol-disulfide exchange and thereby involved in keeping cellular structures reduced and functional [10]. Grx1 has influence on cell differentiation [11] and regulates transcription factors, including NF-kappaB [12, 13]. NF-kappaB exerts an anti-apoptotic function in most cell types, whereas its role in the beta-cell is dependent on its activators. A protective effect against apoptosis induced by TNF-alpha is suggested [14]. Furthermore, researchers demonstrated that Grx1 promotes insulin secretion in MIN6 cells and isolated rat islets [15] while Grx1 knockout resulted in impaired insulin secretion [16]. The second dithiol, Grx2, forms iron-sulfur clusters which act as a redox sensor [17, 18]. As a regulatory mechanism of the redox state in the mitochondria [19] it has protective effects from apoptosis [20]. The monothiol Grx3 can form iron-sulfur clusters [21] as well and is necessary for haem synthesis [22]. It has protective and immunomodulatory effects, too [23, 24]. Grx5 was studied in yeast mutants lacking the enzyme. These featured increased susceptibility to oxidative and osmotic stress. Elevated ROS production, accumulation of iron and inactivation of enzymes requiring Fe-S clusters were noted [25, 26]. These affected enzymes are not only required for glucose processing and thereby insulin secretion, but iron accumulation is also known to induce secondary complications in diabetes [27]. Due to their diverse functions and their substrate specifity, alterations in glutaredoxin activity and expression can have massive impact on cellular pathways. Therefore, a key role in diabetes has been implicated [28]. The metabolically highly active beta-cell suffers from low antioxidant capacity. Several enzymes, including superoxide dismutase, catalase and glutathione peroxidase were shown to be expressed less in mouse islets in comparison to other tissues [29]. Oxidative stress disrupts the physiology of insulin secretion at several stages. GLUT2 (Glucose transporter 2) expression is reduced in rodent models for diabesity [30, 31] and mitochondrial dysfunction [32–34] was reported. Furthermore, oxidative modifications of ATP-sensitive potassium channels as well as hyperpolarization of the cell membrane conducted by ROS can both take influence on insulin secretion [35, 36]. Surprisingly, there are few data regarding glutaredoxins in the islets of diabetic mice. We hypothesized that they play a role in the challenged beta-cell during the onset and progression of diabetes mellitus type 2. Therefore, we screened islets of diabetic db/db mice in comparison to lean db/+ littermates. Homozygote db mice are marked by total leptin resistance due to a receptor mutation [37] and thus develop obesity and diabetes ("diabesity") [38]. We found lower expression of all four glutaredoxins in diabetic mice in comparison to lean controls. The effect was most pronounced for Grx1 and 5, which lead us to further investigate both redoxins. For the first time we detected distinguished differences in Grx expression in the islets of Langerhans in a mouse model for diabetes mellitus type 2 which could be correlated to insulin expression, cell cycle, and ROS production.

Materials and methods

Ethics statement

Animal research was approved by and conducted in accordance with institutional animal welfare officer, Chair of Animal Welfare of the Justus Liebig University Giessen, and Regional Administrative Council Giessen, Veterinary Department, under the code GI20/11-Nr.A18/2010. 3Rs were applied for reducing the number of required mice and reduce potential suffering, enrichment was applied to the IVC. Scoring was done daily. Mice were anaesthetized with ketamin / xylazin i.p. and bled to death by incision of the abdominal aorta before removing the

pancreas and other organs. The ARRIVE Guidelines Checklist (Animal Research: Reporting In Vivo Experiments) is available in the Supporting information section (S1 File).

Animal model

40 male BKS(D)-Leprdb/JOrlRj (db/db) mice and 40 BKS(D)-Leprdb/JOrlRj Témoin (db/+) control mice aged 5 weeks were bought from Charles River (Sulzfeld, Germany) and given one week to adapt to the animal facility. Number of required mice was calculated regarding manifestation rate of diabetes according to literature with type I error of 0.05 and type II error of 0.2. Animals were housed according to institutional guidelines (room temperature 22 ± 0.5°C, 12 hours light / dark cycle, 60% humidity) with tap water and standard diet pellet food (Altromin, Lage, Germany) ad libitum in individually ventilated cages in groups of five mice. Mice were observed from 6 to 18 weeks of age. Blood glucose (Glucometer OneTouch Ultra 2, LifeScan, Neckargemünd, Germany) and body weight were measured weekly. Blood for glucose measurement was collected by puncturing the tip of the tail on conscious animals after overnight fasting. Pancreatectomy for IHC and islet isolation for qRT-PCR were done at 6, 12 and 18 weeks of age. In order to harvest pancreata mice were sedated by narcotic agent (1 ml Ketamine 10%, 0.8 ml Xylazine 2%, 8.2 ml NaCl 0.9%; 0.1 ml / 10 g body weight). Next, the abdominal wall was excised to expose the aorta which was cut to drain the blood before the organ was removed.

Islet isolation

Islets were isolated as described before by our department [39]. Briefly, the extracted pancreas was perfused with 4 mg / ml collagenase B (Roche, Mannheim, Germany) dissolved in 1% Hank's solution (Biochrom, Berlin, Germany) supplemented with 35 ml Hepes buffer (Biochrom, Berlin, Germany), 10 ml Ciprofloxacin, 10 ml Penicillin-Streptomycin, and 1 ml Gentamycin through the ductus pancreaticus. The perfused pancreas was mechanically chopped with scissors before 10 minutes of incubation in collagenase solution at 37°C in a shaking water bath. After every 3 minutes of collagenase digestion the sample was vortexed for 10 seconds. The digested tissue was shaken by hand for two more minutes and the digestion process was eventually stopped by placing the tube containing the tissue on ice and adding cold Hank's solution. Following 3 minutes of centrifugation at 1500 rpm, the supernatant was discarded and the pellet was dissolved in 15% P/FCS dissolved in Medium 199 (Gibco, Karlsruhe, Germany) and fetal bovine serum (biowest, Nuaillé, France) at room temperature. The islets were hand-picked under stereomicroscope and incubated overnight at 37°C to overcome the isolation stress.

Immunohistochemistry

IHC was used for detection of insulin (Dako, Hamburg, Germany), Grx1 (Santa Cruz Biotechnology, USA) and 5 (kindy provided by Prof. Lillig / Dr. Hanschmann as described in [40]), Ki-67 (Dako, Hamburg, Germany) as a marker for proliferation and activated caspase-3 (Cell Signaling, Frankfurt, Germany) as a marker for apoptosis. Pancreata were fixed with Zamboni (paraformaldehyde in picric acid and PBS as described in [41]) for four hours, then washed and stored in PBS supplemented with 18% sucrose solution overnight. Organs were embedded in cryoblock embedding medium (Biosystems, Nunningen, Switzerland) and frozen at -80°C. Sectioning was done using Leica Crysostat CM1850 (Leica, Wetzlar, Germany). Slides were washed with PBS and blocked with 1% donkey serum dissolved in PBS containing 0.3% Triton X-100 (0.3% PBST) for 20 minutes. For Ki-67 staining, antigen retrieval was performed with NaOH 0.09 M for three minutes followed by another wash cycle. Sections were incubated with

primary antibodies diluted in 1% donkey serum dissolved in 0.3% PBST overnight at 4˚C. Secondary antibodies in 5% mouse serum were applied for one hour at room temperature. Nuclei were stained with Hoechst (Calbiochem, Darmstadt, Germany) in 0.1% TRIS buffer pH 7.6 and samples were preserved with ProLong Gold (Invitrogen, Karlsruhe, Germany). Pancreata were entirely sectioned. Sections were assessed for their quality, i.e. structurally damaged ones were not used. Two consecutive sections were regarded as one (results were divided by two for analysis). An interval of 140 μm was maintained between these pairs of slides which were included in the analysis in order to avoid multiple inclusion of islets. When islet area exceeded 140 μm in 12 weeks old db/db mice, double inclusion was carefully avoided by manual comparison of slides. 12 slides per pancreas, including 24 to 384 islets per organ, were observed. Total islet count included in the study was 2221 with 123 islets per mouse on average. Islet count was consistent with the number of islets isolated during islet isolation. Slides were prepared simultaneously in batches during immunohistology for appropriate comparability. For qualitative assessment of redoxin staining patterns in islets, immunostained slides were screened for islets. Images were taken, background staining was removed, and images were converted to gray scale for more effective and accurate comparison. Representative images were then selected manually.

Measurement of islet area and protein expression level

Size of islet area as well as protein expression level of Grx1, Grx5 and insulin were measured by using custom scripts for ImageJ (Wayne Rasband, National Institutes of Health, USA). Images were taken with Leica Application Suite v 3.8.0 using digital microscope camera DFC 420 C (Leica, Wetzlar, Germany) as described before [42]. Software was calibrated to match the images' scale and mean islet area was obtained. For analysis of protein expression level of insulin, Grx1 and 5, gray scaled pictures taken from a batch of simultaneously prepared stainings were normalized by removing background using slides without primary antibodies and calculating mean fluorescent intensity in islets. This resulted in mean grey values ranging from 0 (0%) to 255 (100%). In order to quantify redoxin staining area, the area stained by the antibody against the respective redoxin was set into relation with the area stained by insulin.

RNA isolation, cDNA synthesis and qRT-PCR

Extraction of RNA from harvested islets was done using RNeasy Plus Micro Kit (Qiagen, Düsseldorf, Germany). Total RNA concentration was determined by OD260 nm method using NanoDrop 1000 spectrophotometer (Thermo Scientific, Schwerte, Germany). cDNA was synthesised with SuperScript III Reverse Transcriptase kit (Invitrogen, Darmstadt, Germany). qRT-PR was carried out on Real-Time PCR System StepOnePlus (Applied Biosystems). Each PCR consisted of 10 min denaturation at 95˚C, followed by 40 cycles of denaturation (95˚C, 10 s) and annealing / extension (60˚C, 1 min). Primer concentration for qRT-PCR was 20 pM. Primer (Invitrogen, Darmstadt, Germany) sequences were as follows:

beta-actin (housekeeping):
fwd GTG GGA ATG GGT CAG AAG G, rev GAG GCA TAC AGG GAC AGC A;
INS1:
fwd TAT AAA GCT GGT GGG CAT CC, rev GGG ACC ACA AAG ATG CTG TT;
Grx1:
fwd GAG CAG TTG GAC GCG CTG G, rev CTC GCC ATT GAG GTA CAC TTG C;
Grx5:
fwd GAA GAA GGA CAA GGT GGT GGT CTT C, rev GCA TCT GCA GAA GAA TGT CAC AGC

Relative mRNA expression values were obtained by normalizing CT values of the target genes in comparison with CT values of the housekeeping gene using the delta-CT method.

Measurement of ROS production

Intracellular reactive oxygen species (ROS) production level in isolated islets were detected using 2',7'-dichlorofluorescein diacetate (DCFH-DA) indicator dye (Sigma, Munich, Germany). DCFH-DA is a non-fluorescent, cell-permeable compound which is cleaved by intracellular esterases to 2',7'-dichlorofluorescein (DCFH) and thereby trapped within cells. DCFH is membrane impermeable and a variety of intracellular ROS rapidly oxidize it to the highly fluorescent DCF (2',7'-dichloro-fluorescein) [43, 44]. Isolated islet cells of 24 weeks old animals were categorized in three different groups as untreated control, high glucose treated (20 mM for 2 hours) and TNF-alpha treated (1μM for 15 minutes). The above mentioned samples were incubated in serum-free medium containing 10μM DCFH-DA indicator dye dissolved in dimethylsulfoxide (DMSO) (Sigma, Munich, Germany). After 30 min incubation at 37˚C in the dark, samples were rinsed with pre-warmed serum-free medium and immediately analyzed with confocal laser scanning microscope. Intracellular DCF fluorescence (corrected for background fluorescence) was evaluated in 3600 μm^2 regions of interest using an overlay mask unless otherwise indicated. For fluorescence excitation, the 488 nm band of the argon ion laser of a confocal laser scanning microscope (Leica SP2 AOBS, Bensheim, Germany) was used. Emission was recorded using a longpass LP515 nm filter set. All islet cells per condition were photographed and fluorescence intensities were quantified with Leica Simulator software.

Statistical analysis

Statistical analysis was performed using Graph Pad Prism 5 (GraphPad Software, San Diego, USA) using Mann Whitney test and two-way Anova as appropriate. Data are given as mean values ± SEM, with n denoting the number of experiments unless otherwise indicated. A p-value < 0.05 was considered significant.

Results

A phenotype of diabesity in rodents

The leptin-resistant db mouse was employed for investigation of glutaredoxins in diabetes. It is known that homozygous db mice exhibit a distinct aspect of diabesity. Consecutively, a strong obese and diabetic phenotype was developed during the 12 weeks study period. Homozygous animals constantly showed a significantly higher body weight as well as fasting blood glucose during the observation period from 6 to 18 weeks of age ($p < 0.0001$). At the end of the observation period, homozygotes with 57 g on average were twice as heavy as heterozygotes with 26 g (Fig 1a). Their fasting blood glucose exceeded 200 mg/dl from 13 weeks of age onwards while heterozygotes showed no significant increase from 12 to 18 weeks of age (Fig 1b).

Pathohistomorphic changes with distinct morphology and high cell turnover

After having ensured a strong phenotype in the selected strain of db mice as well as the suitability of heterozygous animals as controls, the histology of their pancreatic islets was examined. Assessment of islet count during islet isolation revealed more islets in db/db animals at all time points ($p < 0.001$ at 6 weeks of age, $p < 0.05$ on average, data not shown). In both groups, lowest pancreatic islet count was observed at the age of 12 weeks. Morphological
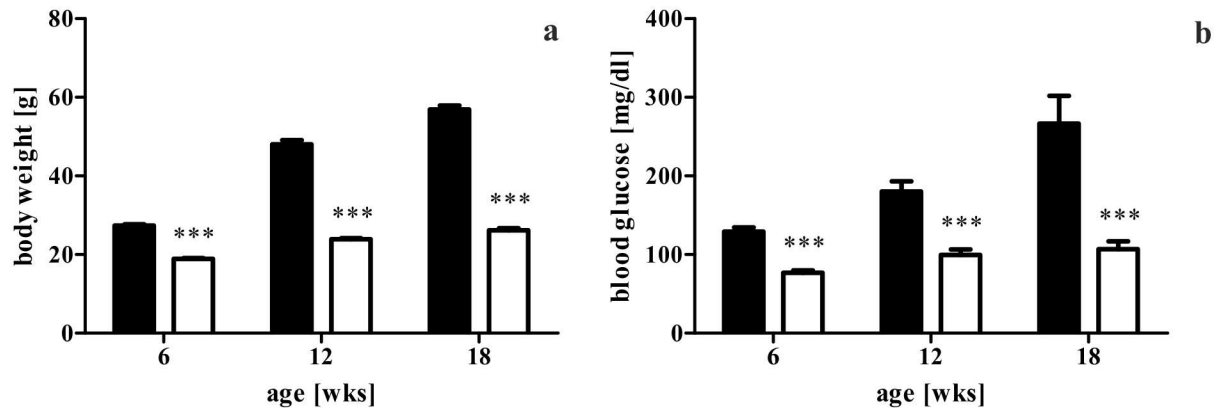
Fig 1. Body weight and fasting blood glucose level of db/db and db/+ mice. (a) Body weight of db/db and db/+ mice. (b) Fasting blood glucose levels of db/db and db/+ mice. Data depicted from 6, 12, and 18 weeks of age, corresponding to pancreatectomy. Values are mean ± SEM (n = 11-40 mice), black bars represent db/db mice, white bars represent db/+ mice, *** denotes $p < 0.0001$.

studies by immunohistology exposed larger islets occuring together with fragmented small ones in homozygotes (Fig 2). At the age of 6 weeks islets of homozygotes were already enlarged but shaped normally (Fig 2a). Larger islets in 12 weeks old db/db mice resulted in vast islet formations (Fig 2f). As homozygotes grew older, small abnormally shaped islets increased in number (Fig 2k). Changes in islets of heterozygotes were more moderate (Fig 2b, 2g and 2l).
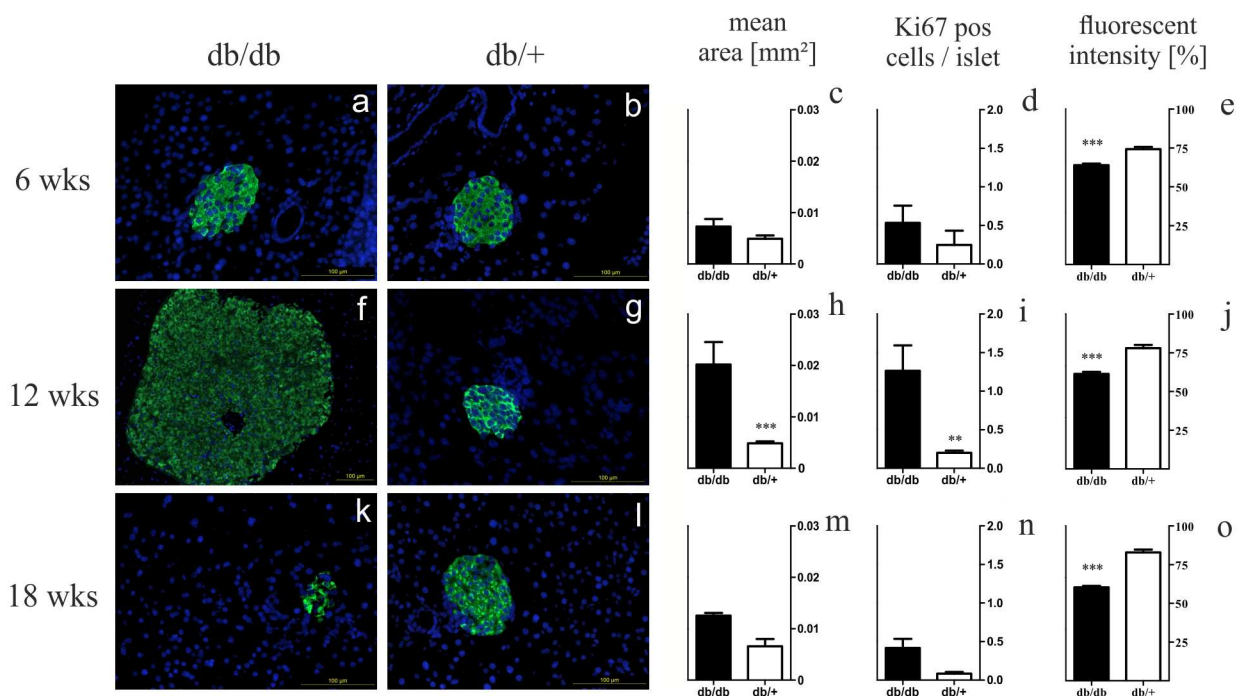

Fig 2. Morphology and quantification of area, proliferation rate, and fluorescent intensity of db/db and db/+ islets. (a, b, f, g, k, l) Representative images taken of immunostained islets at 6, 12 and 18 weeks are shown in comparison (green: insulin, blue: nuclei; bars indicate 100 μm^2). (c, h, m) Quantification of mean islet area as measured with ImageJ corresponding to insulin staining area. (d, i, n) Proliferation of islet cells analyzed by Ki-67 positive cells per islet. (e, j, o) Semiquantitative analysis of insulin staining. Black bars represent db/db mice, white bars represent db/+ mice, n = 3 mice, *** denotes $p < 0.001$, ** denotes $p < 0.005$.

These findings were quantified by measuring islet area in immunostained slides. We found larger mean islet area in db/db animals at all time points with a maximum at 12 weeks ($p < 0.001$ at 12 weeks and $p < 0.005$ on average) (Fig 2c, 2h and 2m). On average, db/db mice had 2.5-fold larger islets. Respectively, islet proliferation was measured by counting of cells positive for Ki-67 staining. We found higher proliferation of db/db islets ($p < 0.005$ at 12 weeks and on average) (Fig 2d, 2i and 2n). Again, a peak was found at 12 weeks in homozygotes, while proliferation decreased in ageing animals of both groups. On average, homozygotes featured a four-fold higher proliferation rate. Slides were also stained against activated caspase-3 and analysed qualitatively. Apoptosis was higher in 6 and 12 weeks old homozygotes in comparison to heterozygotes (data not shown).

Receding insulin content in the islets of Langerhans

Both the phenotype of diabesity as well as the marked histological alterations in db/db mice were accompanied by a depletion of insulin content in islets, as our respective analysis revealed. This loss correlated to the extent of body weight and blood glucose levels of db/db animals. Quantification of insulin staining of immunohistology confirmed the impression of lower insulin content in db/db islets when compared to db/+ specimen ($p < 0.0001$) (Fig 2e, 2j and 2o). Regarding the genetic level, homozygotes showed a 70-fold drop in *INS1* expression from 6 to 18 weeks of age ($p < 0.0001$) (Fig 3a). In comparison to heterozygotes, *INS1* expression was twice as low at 6 and 12 weeks of age ($p < 0.05$) and 45-fold lower at 18 weeks ($p < 0.0001$). Heterozygote expression was declining less markedly.

Marked differences in islet redoxin expression

Our aim was to correlate the witnessed differences between obese, diabetic and lean, non-diabetic mice with changes in glutaredoxin expression. For screening, we assessed the pattern as well as fluorescent intensity of immunohistologically stained islets from 12 weeks old mice of both groups. This timepoint appeared most promising for the observed marked differences in shape, insulin content and proliferation detected in our previous analysis. We discovered visible differences with more dense and extense staining in db/+ animals for all four glutaredoxins, which were most pronounced for Grx1 and 5 (Fig 4).

Reduced glutaredoxin 1 and 5 levels in islets during diabesity

Based on the screening of glutaredoxins in islets, we carried out further analysis for Grx 1 and 5. Staining in db/db islets was more scarce and extended over a smaller area when compared to control islets. Furthermore, Grx5 staining patterns were more intense and more extensive than Grx1 patterns. Findings were confirmed by semiquantitative analysis of Grx fluorescent intensity as well as quantification of Grx to insulin staining ratio (Fig 5). Control islets featured higher Grx fluorescent intensity and Grx to insulin ratio for both redoxins and all time points. Grx5 was the redoxin with higher expression. To confirm the findings on the genome level, gene expression of *Grx1* and *5* was analysed by qRT-PCR in isolated islets. Corresponding to higher fluorescent intensity and area, heterozygotes showed higher gene expression ($p < 0.0001$ at 6 and 12 weeks) for *Grx1* at all time points (Fig 3b). In homozygote islets, a nadir was found at 12 weeks, while expression im heterozygote islets was stable. Analysis of *Grx5* expression revealed a significant decrease ($p < 0.0001$) in both db/db and db/+ animals with controls exhibiting higher expression at all time points ($p < 0.0001$ at 6 and 12 weeks) (Fig 3c). qRT-PCR revealed a markedly higher expression of *Grx5* when compared to *Grx1*.
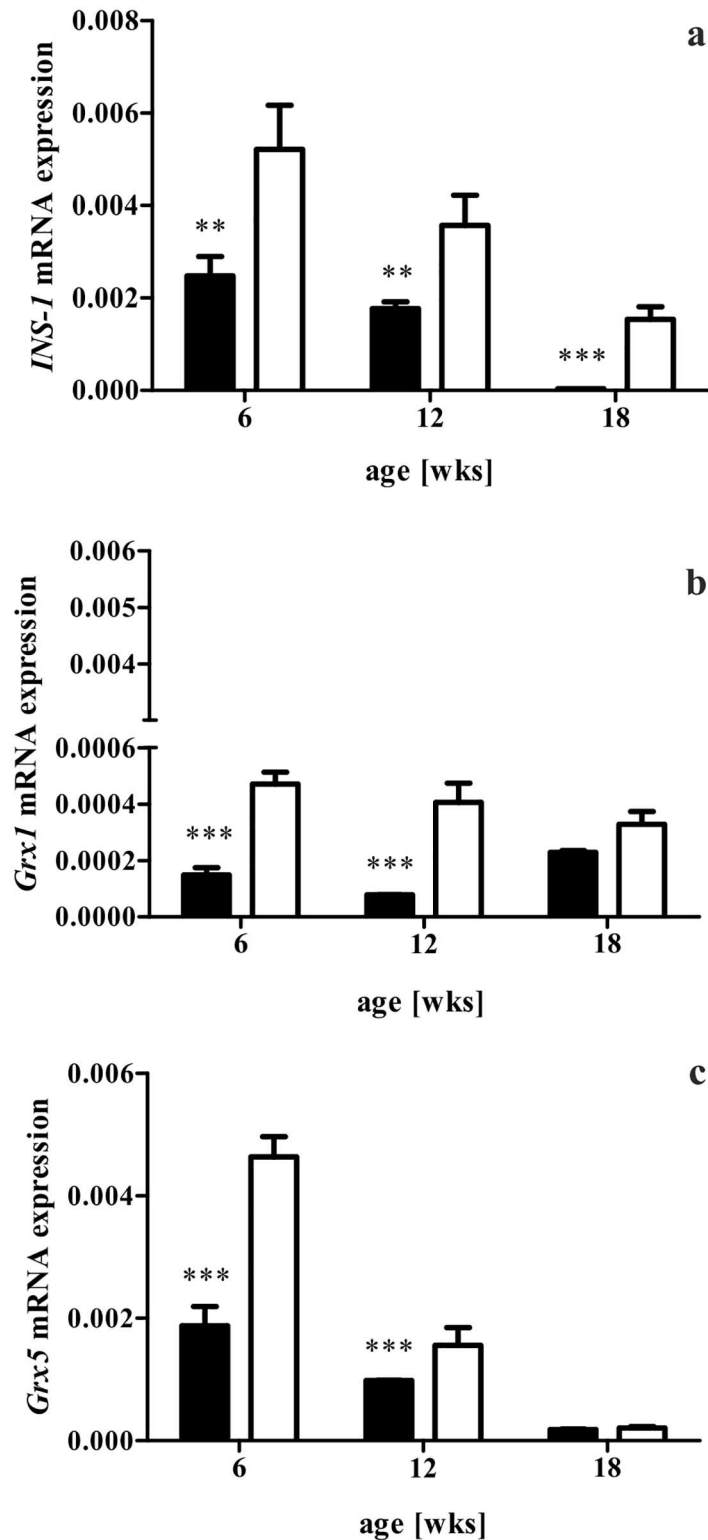
Fig 3. Gene expression of *INS1*, *Grx1*, and *Grx5* in db/db and db/+ islets. Gene expression was evaluated by qRT-PCR. (a) *INS1* expression declined in both groups of mice in relation to their age, but controls exhibited significantly higher expression levels at all time points. (b) *Grx1* expression was higher in db/+ mice at all time points. A slight decrease in controls was observed, while db/db animals featured a gap at 12 weeks of age. (c) *Grx5* expression decreased in both groups with age with higher levels in db/+ islets.

Values are mean ± SEM (n = 4—6 mice) and normalized with beta-actin, black bars represent db/db mice, white bars represent db/+ mice, *** denotes $p < 0.0001$, ** denotes $p < 0.005$.

Enhanced ROS production in Grx-deficient islets

In order to further evaluate the significance of Grx-deficiency in mouse islets in diabetes, we analyzed ROS production level in isolated pancreatic islets using DCF staining. It was evaluated in untreated islets as well as islets pretreated with high glucose and TNF-alpha in order to stimulate hyperglycaemic and inflammatory stress as apparent during diabetes mellitus type 2. Isolated pancreatic islets from homozygous mice indicated higher ROS production level without any stimulation as well as upon treatment with either glucose or TNF-alpha compared to heterozygotes ($p < 0.0001$). Both groups showed an elevation in ROS content upon treatment with either glucose or TNF-alpha, but with a markedly higher level in db/db islets (Fig 6).

Discussion

The course of diabetes mellitus type 2 is highly dependent on the preservation of a healthy beta-cell mass and insulin secretion capacity, which both are notably impaired by oxidative stress and disturbed redox signaling [45]. It was previously shown that the Grx system has positive impact on insulin secretion [16, 46, 47]. Furthermore, tissue-specific expression of Grx was reported [48]. Plasmatic Grx activity differs between healthy subjects and patients suffering from diabetes mellitus type 2 [49]. Evidence for a protective role of the Grx system in the diabetic metabolism has arisen [50–54], but its exact significance for the beta-cell is still unknown. Thus, the aim of this study was to evaluate the relevance of the glutathione-dependent oxidoreductase system as a potential protection machinery in an in vitro model for diabetes mellitus type 2. A high level of oxidative phosphorylation is mandatory for the metabolically active beta-cell, especially when challenged by metabolic stress. As a result, mitochondrial ROS are considered a requirement for unimpaired insulin secretion [55, 56]. However, it is accepted that an abundance of ROS induces oxidative stress, exerts detrimental effects on cellular structures and proteins, and disturbs redox signaling. Accordingly, permanent excess of ROS is seen as noxious to insulin secretion [57]. Elevated ROS production in islets of
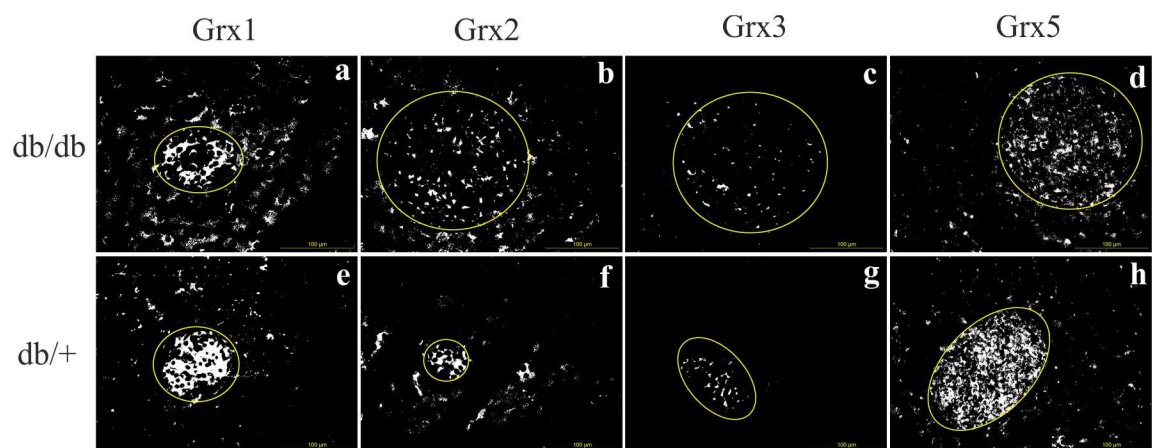

Fig 4. Qualitative comparison of the Grx system in db/db and db/+ islets. Representative monochrome pictures of Grx staining pattern captured of islets of 12 weeks old db/db and db/+ mice. (a, e) Grx1, (b, f) Grx2, (c, g) Grx3, (d, h) Grx5. Staining patterns suggested higher expression in db/+ mice. The difference was most pronounced for Grx1 and 5. 200x, yellow circles indicate islets, bars indicate 100 μm^2.
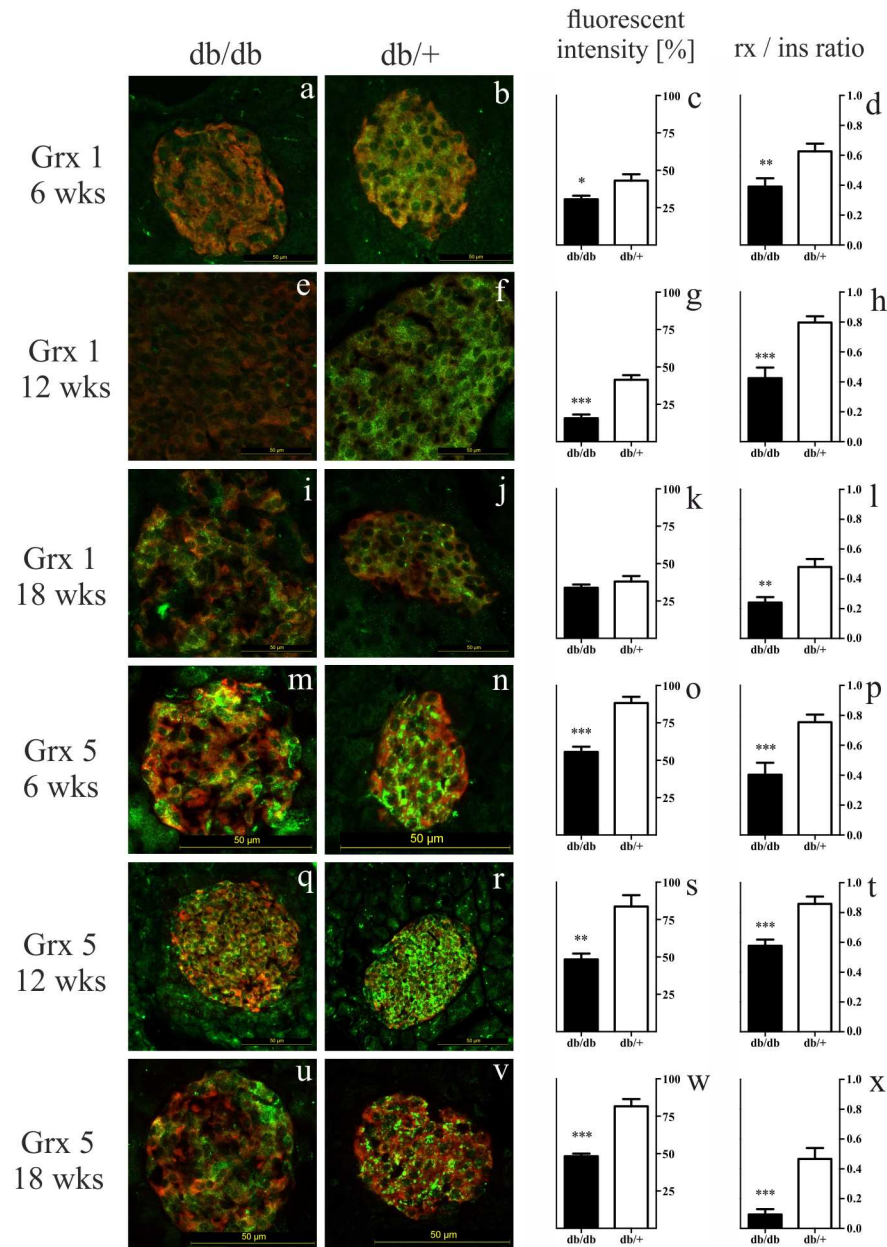
Fig 5. Representative images of Grx1 and 5 staining, quantification of Grx to insulin ratio, and fluorescent intensity of db/db and db/+ islets. (a, b, e, f, i, j, m, n, q, r, u, v) Representative images taken of immunostained islets at 6, 12 and 18 weeks are shown in comparison (green: Grx1 / 5, red: insulin, bars indicate 50 μm^2). (c, g, k, o, s, w) Semiquantitative analysis of Grx1 / 5 staining. (d, h, l, p, t, x) Quantification of Grx 1 / 5 to insulin staining ratio. Black bars represent db/db mice, white bars represent db/+ mice, n = 3 mice, *** denotes $p < 0.0001$, ** denotes $p < 0.005$, * denotes $p < 0.05$.

diabetic rodents were confirmed by others [58], and overexpression of radical-scavenging enzymes resulted in protection of ROS-mediated induction of diabetes [59]. The beta-cell is especially prone to oxidative damage for its low expression of enzymes such as catalase and glutathione peroxidase, which are mainly involved in detoxification of H_2O_2 [29]. The glutaredoxin system has been proven to be expressed in mice islets [48] and may represent an
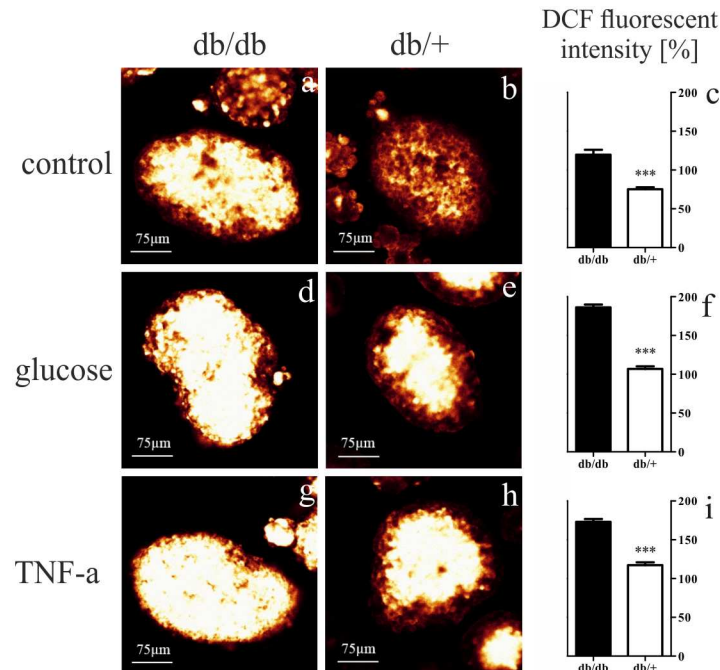
Fig 6. Representative images of ROS measurements and quantification in islets of db/db and db/+ mice. (a, b, d, e, g, h) Representative images show DCF stained pancreatic islets without any treatment as well as upon treatment with either glucose or TNF-alpha (bars represent 75 µm). (c, f, i) Quantification of DCT fluorescence intensity revealed significantly higher ROS production in db/db islets with a more pronounced rise after exposure to high glucose and TNF-alpha treatment in comparison to db/+ islets. Values are mean ± SEM (n = 54—139 islets), black bars represent db/db islets, white bars represent db/+ islets, *** denotes $p < 0.0001$.

important alternative pathway in detoxification of ROS for the beta-cell. The four mammalian glutaredoxins are located in the major cellular compartments [8, 21, 26, 60] and are thereby involved in a broad range of functions. Thus, it is acknowledged that they feature varying expression patterns and activity when the beta-cell is challenged by metabolic stress. In the present study, we identified significant differences in Grx expression between diabese mice and lean controls for all four oxidoreductases, which were most pronounced for the mainly cytoplasmic Grx1 as well as the mitochondrial Grx5. Our data indicate that Grx1 expression correlated negatively with average size of pancreatic islets as well as proliferation rate, and positively with islet count in homozygotes. Grx1 protein and mRNA expression were elevated at 6 and 18 weeks when beta-cell turnover was at its minimum. At these time points homozygous mice featured high islet count and small islets with low proliferation rate. By contrast, we found reduced mRNA and protein expression of Grx1 at 12 weeks when islet count was low, but islets were large and showed elevated proliferation. Furthermore, a correlation was found between higher and stable expression in heterozygotes and less apoptosis of islet cells, elevated insulin expression and stable blood glucose levels when compared to homozygotes. These observations support the anti-apoptotic [61, 62] and pro-proliferative role [11] of Grx1. Grx1 is a major catalyst of post-translational modification of proteins via de-glutathionylation [61, 63], reversing detrimental glutathionylation by ROS. Among its targets are NF-kappaB, a key regulator of apoptosis [64], and PKC-alpha [65]. Previous studies suggest a positive impact of PKC-alpha on insulin secretion via maintenance of calcium channels [66, 67]. Further, Grx1 restores aldose reductase [68], an enzyme which is required for glucose processing if

hexokinase is saturated due to glucose overload. A recent study linked Grx to adenosine monophosphate-activated protein kinase (AMPK) activation and thereby stabilization of insulin secretion [54]. Consequently, Grx1 might support generation of new islets as well as growth of pre-existing islets, and further sustain islet metabolic activity in attempt to maintain glucose homeostasis and preserve insulin secretion capacity. In this study, Grx5 featured a significant reduction in both groups of mice, which was markedly more pronounced in db/db animals and correlated with fading insulin expression and rising blood glucose levels. The Grx5 enzyme is an important actor in composition of iron-sulfur clusters in the mitochondria [26]. Therefore, it is essential for a broad range of enzymes relying on these clusters, among which numerous have relevance for the respiratory chain [26]. Thus, the connection between Grx5 and oxidative phosphorylation might explain the co-occurrence of reduced insulin as well as Grx5 expression in this study. It has been reported that Grx5-deficiency increases the susceptibility to oxidative stress [25]. Furthermore, a lack of Grx5 enzyme was also correlated to cellular iron overload [69]. Iron is known to catalyze ROS production and thereby mediate apoptosis [70]. The link between metabolic stress and iron metabolism was shown in an in vivo model for diabetes mellitus type 2 with defective iron channels which featured stronger beta-cell viability [71]. Also, iron chelator treatment and dietary iron restriction had beneficial effects on glucose homeostasis in rodents [72]. Therefore, Grx5 might play a key role in maintaining mitochondrial functionality and prevent detrimental impact of iron accumulation. At the present time, the exact significance of reduced Grx1 and 5 levels in diabese db/db mice remains to be studied. Functional experiments will elucidate whether reduced redoxin levels are cause or result of impaired insulin secretion in islets of diabese animals. Regulators and effectors of islet redoxins have to be identified and modulation of redoxin expression should
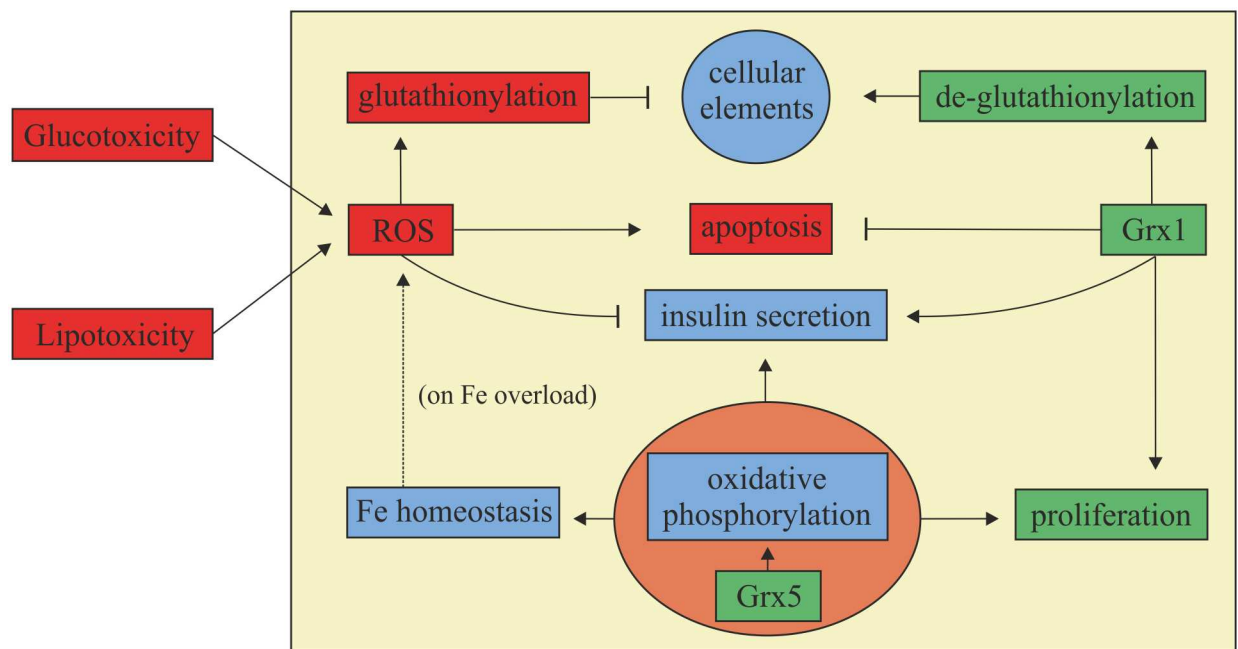

Fig 7. Summary. Both gluco- and lipotoxicity are extracellular promoters of ROS generation. ROS are harmful to cellular elements as they catalyze their glutathionylation. When the cell's antioxidant capacity is depleted, cell death occurs. Regarding the beta-cell, ROS impair insulin secretion. Grx1 and 5 wield protective properties. Grx1 is a major actor in de-glutathionylation, thereby reversing the harmful effects of ROS on its targets, exerting anti-apoptotic and pro-proliferative effects, and preserving insulin secretion. Grx5 has impact on the respiratory chain and cellular iron homeostasis by transferring iron-sulfur clusters to respective apoproteins. Hence, it supports cell viability and function, allows proliferation and counteracts iron accumulation which would promote ROS formation.

be investigated regarding its influence on islet viability and metabolic activity. Further, immunohistological analysis in this study was limited by a low number of mice (n = 3). However, an appropriate amount of islets per animal was used for analysis and results were consistent among animals. Moreover, genome analysis via mRNA expression was carried out in 4 to 6 mice per timepoint and results were consistent with protein analysis.

Conclusion

In conclusion, our findings demonstrate a correlation between glutaredoxins and dysfunction of the islets of Langerhans in a mouse model for diabesity, which has not been described before. We propose that deficiency of Grx1 and 5 is connected to impaired insulin secretion and beta-cell decay in diabetes mellitus type 2. A summary of the obeserved correlations in reference to literature is given in Fig 7.

Supporting information

S1 File. The ARRIVE guidelines checklist. The ARRIVE Guidelines Checklist (Animal Research: Reporting In Vivo Experiments) was followed and is available.
(PDF)

Author Contributions

Conceptualization: TL.

Data curation: SFP.

Formal analysis: SFP FS.

Funding acquisition: TL.

Investigation: SFP FS.

Methodology: SFP FS HS TL.

Project administration: SFP TL.

Resources: HS TL.

Software: SFP.

Supervision: TL.

Validation: TL.

Visualization: SFP.

Writing – original draft: SFP.

Writing – review & editing: SFP FS TL.

References

1. Robertson RP, Harmon J, Tran PO, Tanaka Y, Takahashi H. Glucose toxicity in beta-cells: type 2 diabetes, good radicals gone bad, and the glutathione connection. Diabetes. 2003; 52(3):581–7. https://doi.org/10.2337/diabetes.52.3.581 PMID: 12606496

2. American Diabetes Association. Report of the Expert Committee on the Diagnosis and Classification of Diabetes Mellitus. Diabetes Care. 2003; 26:Suppl 1:S5–20. PMID: 12502614

3. DeFronzo RA. Pathogenesis of type 2 diabetes mellitus. Med Clin North Am. 2004; 88(4):787–835. https://doi.org/10.1016/j.mcna.2004.04.013 PMID: 15308380

4. Robertson RP, Harmon J, Tran PO, Poitout V. Beta-cell glucose toxicity, lipotoxicity, and chronic oxidative stress in type 2 diabetes. Diabetes. 2004; 53:Suppl 1:S119–24. https://doi.org/10.2337/diabetes.53.2007.S119 PMID: 14749276

5. Ullrich V, Kissner R. Redox signaling: bioinorganic chemistry at its best. J Inorg Biochem. 2006; 100 (12):2079–86. https://doi.org/10.1016/j.jinorgbio.2006.09.019 PMID: 17095095

6. Holmgren A. Hydrogen donor system for Escherichia coli ribonucleoside-diphosphate reductase dependent upon glutathione. Proc Natl Acad Sci U S A. 1976; 73(7):2275–9. https://doi.org/10.1073/pnas.73.7.2275 PMID: 7783

7. Holmgren A. Glutathione-dependent synthesis of deoxyribonucleotides. Purification and characterization of glutaredoxin from Escherichia coli. J Biol Chem. 1979; 254(9):3664–71. PMID: 372193

8. Lundberg M, Fernandes AP, Kumar S, Holmgren A. Cellular and plasma levels of human glutaredoxin 1 and 2 detected by sensitive ELISA systems. Biochem Biophys Res Commun. 2004; 319(3):801–9. https://doi.org/10.1016/j.bbrc.2004.04.199 PMID: 15184054

9. Pai HV, Starke DW, Lesnefsky EJ, Hoppel CL, Mieyal JJ. What is the functional significance of the unique location of glutaredoxin 1 (GRx1) in the intermembrane space of mitochondria? Antioxid Redox Signal. 2007; 9(11):2027–33. https://doi.org/10.1089/ars.2007.1642 PMID: 17845131

10. Holmgren A. Thioredoxin and glutaredoxin systems. J Biol Chem. 1989; 264(24):13963–6. PMID: 2668278

11. Takashima Y, Hirota K, Nakamura H, Nakamura T, Akiyama K, Cheng FS, et al. Differential expression of glutaredoxin and thioredoxin during monocytic differentiation. Immunol Lett. 1999; 68(2-3):397–401. https://doi.org/10.1016/S0165-2478(99)00087-5 PMID: 10424449

12. Hirota K, Matsui M, Murata M, Takashima Y, Cheng FS, Itoh T, et al. Nucleoredoxin, glutaredoxin, and thioredoxin differentially regulate NF-kappaB, AP-1, and CREB activation in HEK293 cells. Biochem Biophys Res Commun. 2000; 274(1):177–82. https://doi.org/10.1006/bbrc.2000.3106 PMID: 10903915

13. Daily D, Vlamis-Gardikas A, Offen D, Mittelman L, Melamed E, Holmgren A, et al. Glutaredoxin protects cerebellar granule neurons from dopamine-induced apoptosis by activating NF-kappa B via Ref-1. J Biol Chem. 2001; 276(2):1335–44. https://doi.org/10.1074/jbc.M008121200 PMID: 11035035

14. Kim S, Millet I, Kim HS, Kim JY, Han MS, Lee MK, et al. NF-kappa B prevents beta cell death and autoimmune diabetes in NOD mice. Proc Natl Acad Sci U S A. 2007; 104(6):1913–8. https://doi.org/10.1073/pnas.0610690104 PMID: 17267600

15. Ivarsson R, Quintens R, Dejonghe S, Tsukamoto K, in't Veld P, Renström E, et al. Redox control of exocytosis: regulatory role of NADPH, thioredoxin, and glutaredoxin. Diabetes. 2005; 54(7):2132–42. https://doi.org/10.2337/diabetes.54.7.2132 PMID: 15983215

16. Reinbothe TM, Ivarsson R, Li DQ, Niazi O, Jing X, Zhang E, et al. Glutaredoxin-1 mediates NADPH-dependent stimulation of calcium-dependent insulin secretion. J Mol Endocrinol. 2009; 23(6):893–900. https://doi.org/10.1210/me.2008-0306

17. Berndt C, Hudemann C, Hanschmann EM, Axelsson R, Holmgren A, Lillig CH. How does iron-sulfur cluster coordination regulate the activity of human glutaredoxin 2? Antioxid Redox Signal. 2007; 9 (1):151–7. PMID: 17115894

18. Lillig CH, Berndt C, Vergnolle O, Lönn ME, Hudemann C, Bill E, et al. Characterization of human glutaredoxin 2 as iron-sulfur protein: A possible role as redox sensor. Proc Natl Acad Sci U S A. 2005; 102 (23):8168–73. https://doi.org/10.1073/pnas.0500735102 PMID: 15917333

19. Beer SM, Taylor ER, Brown SE, Dahm CC, Costa NJ, Runswick MJ, et al. Glutaredoxin 2 catalyzes the reversible oxidation and glutathionylation of mitochondrial membrane thiol proteins: implications for mitochondrial redox regulation and antioxidant DEFENSE. J Biol Chem. 2004; 279(46):47939–51. https://doi.org/10.1074/jbc.M408011200 PMID: 15347644

20. Enoksson M, Fernandes AP, Prast S, Lillig CH, Holmgren A, Orrenius S. Overexpression of glutaredoxin 2 attenuates apoptosis by preventing cytochrome c release. Biochem Biophys Res Commun. 2005; 327(3):774–9. https://doi.org/10.1016/j.bbrc.2004.12.067 PMID: 15649413

21. Haunhorst P, Berndt C, Eitner S, Godoy JR, Lillig CH. Characterization of the human monothiol glutaredoxin 3 (PICOT) as iron-sulfur protein. Biochem Biophys Res Commun. 2010; 394(2):372–6. https://doi.org/10.1016/j.bbrc.2010.03.016 PMID: 20226171

22. Haunhorst P, Hanschmann E, Bräutigam L, Stehling O, Hoffmann B, Mühlenhoff U, et al. Crucial function of vertebrate glutaredoxin 3 (PICOT) in iron homeostasis and hemoglobin maturation. Mol Biol Cell. 2013; 24(12):1895–903. https://doi.org/10.1091/mbc.E12-09-0648 PMID: 23615448

23. Witte S, Villalba M, Bi K, Liu Y, Isakov N, Altman A. Inhibition of the c-Jun N-terminal kinase/AP-1 and NF-kappaB pathways by PICOT, a novel protein kinase C-interacting protein with a thioredoxin homology domain. J Biol Chem. 2000; 275(3):1902–9. https://doi.org/10.1074/jbc.275.3.1902 PMID: 10636891

24. Kato N, Motohashi S, Okada T, Ozawa T, Mashima K. PICOT, protein kinase C theta-interacting protein, is a novel regulator of FcepsilonRI-mediated mast cell activation. Cell Immunol. 2008; 251(1):62–7. https://doi.org/10.1016/j.cellimm.2008.04.005 PMID: 18479680

25. Rodríguez-Manzaneque MT, Ros J, Cabiscol E, Sorribas A, Herrero E. Grx5 glutaredoxin plays a central role in protection against protein oxidative damage in Saccharomyces cerevisiae. Mol Cell Biol. 1999; 19(12):8180–90. https://doi.org/10.1128/MCB.19.12.8180 PMID: 10567543

26. Rodríguez-Manzaneque MT, Tamarit J, Bellí G, Ros J, Herrero E. Grx5 is a mitochondrial glutaredoxin required for the activity of iron/sulfur enzymes. Mol Biol Cell. 2002; 13(4):1109–21. https://doi.org/10.1091/mbc.01-10-0517 PMID: 11950925

27. Ikeda Y, Enomoto H, Tajima S, Izawa-Ishizawa Y, Kihira Y, Ishizawa K, et al. Dietary iron restriction inhibits progression of diabetic nephropathy in db/db mice. Am J Physiol Renal Physiol. 2013; 304(7): F1028–36. https://doi.org/10.1152/ajprenal.00473.2012

28. Hanschmann EM, Godoy JR, Berndt C, Hudemann C, Lillig CH. Thioredoxins, glutaredoxins, and peroxiredoxins–molecular mechanisms and health significance: from cofactors to antioxidants to redox signaling. Antioxid Redox Signal. 2013; 19(13):1539–605. https://doi.org/10.1089/ars.2012.4599 PMID: 23397885

29. Lenzen S, Drinkgern J, Tiedge M. Low antioxidant enzyme gene expression in pancreatic islets compared with various other mouse tissues. Free Radic Biol Med. 1996; 20(3):463–6. https://doi.org/10.1016/0891-5849(96)02051-5 PMID: 8720919

30. Thorens B, Wu YJ, Leahy JL, Weir GC. The loss of GLUT2 expression by glucose-unresponsive beta cells of db/db mice is reversible and is induced by the diabetic environment. J Clin Invest. 1992; 90 (1):77–85. https://doi.org/10.1172/JCI115858 PMID: 1634622

31. Kluth O, Mirhashemi F, Scherneck S, Kaiser D, Kluge R, Neschen S, et al. Dissociation of lipotoxicity and glucotoxicity in a mouse model of obesity associated diabetes: role of forkhead box O1 (FOXO1) in glucose-induced beta cell failure. Diabetologia. 2011; 54(3):605–16. https://doi.org/10.1007/s00125-010-1973-8 PMID: 21107520

32. Anello M, Lupi R, Spampinato D, Piro S, Masini M, Boggi U, et al. Functional and morphological alterations of mitochondria in pancreatic beta cells from type 2 diabetic patients. Diabetologia. 2005; 48 (2):282–9. https://doi.org/10.1007/s00125-004-1627-9 PMID: 15654602

33. Tretter L, Adam-Vizi V. Inhibition of Krebs Cycle Enzymes by Hydrogen Peroxide: A Key Role of a-Ketoglutarate Dehydrogenase in Limiting NADH Production under Oxidative Stress. J Neurosci. 2000; 20 (24):8972–9. PMID: 11124972

34. Hasan NM, Longacre MJ, Stoker SW, Boonsaen T, Jitrapakdee S, Kendrick MA, et al. Impaired anaplerosis and insulin secretion in insulinoma cells caused by small interfering RNA-mediated suppression of pyruvate carboxylase. J Biol Chem. 2008; 283(42):28048–59. https://doi.org/10.1074/jbc.M804170200 PMID: 18697738

35. Islam MS, Berggren PO, Larsson O. Sulfhydryl oxidation induces rapid and reversible closure of the ATP-regulated K+ channel in the pancreatic beta-cell. FEBS Lett. 1993; 319(1-2):128–32. https://doi.org/10.1016/0014-5793(93)80051-U PMID: 8454044

36. Krippeit-Drews P, Lang F, Häussinger D, Drews G. H2O2 induced hyperpolarization of pancreatic B-cells. Pflugers Arch. 1994; 426(6):552–4. https://doi.org/10.1007/BF00378534 PMID: 8052526

37. Chen H, Charlat O, Tartaglia LA, Woolf EA, Weng X, Ellis SJ, et al. Evidence that the diabetes gene encodes the leptin receptor: identification of a mutation in the leptin receptor gene in db/db mice. Cell. 1996; 84(3):491–5. https://doi.org/10.1016/S0092-8674(00)81294-5 PMID: 8608603

38. Hummel KP, Dickie MM, Coleman DL. Diabetes, a new mutation in the mouse. Science. 1966; 153 (3740):1127–8. https://doi.org/10.1126/science.153.3740.1127 PMID: 5918576

39. Lai Y, Schneider D, Kidszun A, Hauck-Schmalenberger I, Breier G, Brandhorst D, et al. Vascular endo-thelial growth factor increases functional beta-cell mass by improvement of angiogenesis of isolated human and murine pancreatic islets. Transplantation. 2005; 79(11):1530–6. PMID: 15940042

40. Hanschmann EM. Thioredoxin family proteins in physiology and disease.; 2011. Dissertation.

41. Stefanini M, De Martino C, Zamboni L. Fixation of ejaculated spermatozoa for electron microscopy. Nature. 1967; 216(173–174).

42. Kilimnik G, Kim A, Jo J, Miller K, Hara M. Quantification of pancreatic islet distribution in situ in mice. Am J Physiol Endocrinol Metab. 2009; 297(6):E1331–8. https://doi.org/10.1152/ajpendo.00479.2009 PMID: 19808908

43. Sauer H, Engel S, Milosevic N, Sharifpanah F, Wartenberg M. Activation of AMP-kinase by AICAR induces apoptosis of DU-145 prostate cancer cells through generation of reactive oxygen species and activation of c-Jun N-terminal kinase. Int J Oncol. 2012; 2(2):501–8.

44. Bolt HN, Hengstler JG, Stewart J. Analyses of reactive oxygen species. EXCLI J. 2009; 8:241–5.

45. Evans JL, Goldfine ID, Maddux BA, Grodsky GM. Oxidative stress and stress-activated signaling path-ways: a unifying hypothesis of type 2 diabetes. Endocr Rev. 2002; 23(5):599–622. https://doi.org/10.1210/er.2001-0039 PMID: 12372842

46. Liu X, Han S, Yang Y, Kang J, Wu J. Glucose-induced glutathione reduction in mitochondria is involved in the first phase of pancreatic beta-cell insulin secretion. Biochem Biophys Res Commun. 2015; 464 (3):730–6. https://doi.org/10.1016/j.bbrc.2015.07.016 PMID: 26164230

47. Takahashi HK, Santos LR, Roma LP, Duprez J, Broca C, Wojtusciszyn A, et al. Acute nutrient regula-tion of the mitochondrial glutathione redox state in pancreatic beta-cells. Biochem J. 2014; 460(3):411–23. https://doi.org/10.1042/BJ20131361 PMID: 24678915

48. Godoy JR, Funke M, Ackermann W, Haunhorst P, Oesteritz S, Capani F, et al. Redox atlas of the mouse. Immunohistochemical detection of glutaredoxin-, peroxiredoxin-, and thioredoxin-family pro-teins in various tissues of the laboratory mouse. Biochim Biophys Acta. 2011; 1810(1):2–92. https://doi.org/10.1016/j.bbagen.2010.05.006 PMID: 20682242

49. Du Y, Zhang H, Montano S, Hegestam J, Ekberg NR, Holmgren A, et al. Plasma glutaredoxin activity in healthy subjects and patients with abnormal glucose levels or overt type 2 diabetes. Acta Diabetol. 2013; 9(2):225–32.

50. Shelton MD, Kern TS, Mieyal JJ. Glutaredoxin regulates nuclear factor kappa-B and intercellular adhe-sion molecule in Müller cells: model of diabetic retinopathy. J Biol Chem. 2007; 282(17):12467–74. https://doi.org/10.1074/jbc.M610863200 PMID: 17324929

51. Lekli I, Mukherjee S, Ray D, Gurusamy N, Kim YH, Tosaki A, et al. Functional recovery of diabetic mouse hearts by glutaredoxin-1 gene therapy: role of Akt-FoxO-signaling network. Gene Ther. 2010; 17(4):478–85. https://doi.org/10.1038/gt.2010.9 PMID: 20182516

52. Di Simplicio P, de Giorgio LA, Cardaioli E, Lecis R, Miceli M, Rossi R, et al. Glutathione, glutathione uti-lizing enzymes and thioltransferase in platelets of insulin-dependent diabetic patients: relation with platelet aggregation and with microangiopatic complications. Eur J Clin Invest. 1995; 25(9):665–9. https://doi.org/10.1111/j.1365-2362.1995.tb01983.x PMID: 7498240

53. Seghieri G, di Simplicio P, de Giorgio LA, Anichini R, Alberti L, Franconi F. Relationship between meta-bolic glycaemic control and platelet content of glutathione and its related enzymes, in insulin-dependent diabetes mellitus. Clin Chim Acta. 2000; 299(1-2):109–17. https://doi.org/10.1016/S0009-8981(00)00283-7 PMID: 10900297

54. Dong K, M W, Liu X, Huang Y, Zhang D, Wang Y, et al. Glutaredoxins concomitant with optimal ROS activate AMPK through S-glutathionylation to improve glucose metabolism in type 2 diabetes. Free Radic Biol Med. 2016; 101:334–47. https://doi.org/10.1016/j.freeradbiomed.2016.10.007 PMID: 27743883

55. Leloup C, Tourrel-Cuzin C, Magnan C, Karaca M, Castel J, Carneiro L, et al. Mitochondrial reactive oxy-gen species are obligatory signals for glucose-induced insulin secretion. Diabetes. 2009; 58(3):673–81. https://doi.org/10.2337/db07-1056 PMID: 19073765

56. Munhoz AC, Riva P, Simões D, Curi R, Carpinelli AR. Control of Insulin Secretion by Production of Reac-tive Oxygen Species: Study Performed in Pancreatic Islets from Fed and 48-Hour Fasted Wistar Rats. PLoS One. 2016; 11(6):e0158166. https://doi.org/10.1371/journal.pone.0158166 PMID: 27362938

57. Li N, Li B, Brun T, Deffert-Delbouille C, Mahiout Z, Daali Y, et al. NADPH oxidase NOX2 defines a new antagonistic role for reactive oxygen species and cAMP/PKA in the regulation of insulin secretion. Dia-betes. 2012; 61(11):2842–50. https://doi.org/10.2337/db12-0009 PMID: 22933115

58. Bindokas VP, Kuznetsov A, Sreenan S, Polonsky KS, Roe MW, Philipson LH. Visualizing superoxide production in normal and diabetic rat islets of Langerhans. J Biol Chem. 2003; 278(11):9796–801. https://doi.org/10.1074/jbc.M206913200 PMID: 12514170

59. Kubisch HM, Wang J, Bray TM, Phillips JP. Targeted overexpression of Cu/Zn superoxide dismutase protects pancreatic beta-cells against oxidative stress. Diabetes. 1997; 46(10):1563–6. https://doi.org/10.2337/diabetes.46.10.1563 PMID: 9313750

60. Lundberg M, Johansson C, Chandra J, Enoksson M, Jacobsson G, Ljung J, et al. Cloning and expression of a novel human glutaredoxin (Grx2) with mitochondrial and nuclear isoforms. J Biol Chem. 2001; 276(28):26269–75. https://doi.org/10.1074/jbc.M011605200 PMID: 11297543

61. Chrestensen CA, Starke DW, Mieyal JJ. Acute cadmium exposure inactivates thioltransferase (Glutaredoxin), inhibits intracellular reduction of protein-glutathionyl-mixed disulfides, and initiates apoptosis. J Biol Chem. 2000; 275(34):26556–65. https://doi.org/10.1074/jbc.M004097200 PMID: 10854441

62. Murata H, Ihara Y, Nakamura H, Yodoi J, Sumikawa K, Kondo T. Glutaredoxin exerts an antiapoptotic effect by regulating the redox state of Akt. J Biol Chem. 2003; 278(50):50226–33. https://doi.org/10.1074/jbc.M310171200 PMID: 14522978

63. Gravina SA, Mieyal JJ. Thioltransferase is a specific glutathionyl mixed disulfide oxidoreductase. Biochemistry. 1993; 32(13):3368–76. https://doi.org/10.1021/bi00064a021 PMID: 8461300

64. Reynaert NL, van der Vliet A, Guala AS, McGovern T, Hristova M, Pantano C, et al. Dynamic redox control of NF-kappaB through glutaredoxin-regulated S-glutathionylation of inhibitory kappaB kinase beta. Proc Natl Acad Sci U S A. 2006; 103(35):13086–91. https://doi.org/10.1073/pnas.0603290103 PMID: 16916935

65. Ward NE, Stewart JR, Ioannides CG, O'Brian CA. Oxidant-induced S-glutathiolation inactivates protein kinase C-alpha (PKC-alpha): a potential mechanism of PKC isozyme regulation. Biochemistry. 2000; 39(33):10319–29. https://doi.org/10.1021/bi000781g PMID: 10956021

66. Warwar N, Efendic S, Ostenson CG, Haber EP, Cerasi E, Nesher R. Dynamics of glucose-induced localization of PKC isoenzymes in pancreatic beta-cells: diabetes-related changes in the GK rat. Diabetes. 2006; 55(3):590–9. https://doi.org/10.2337/diabetes.55.03.06.db05-0001 PMID: 16505220

67. Arkhammar P, Juntti-Berggren L, Larsson O, Welsh M, Nånberg E, Sjöholm A, et al. Protein kinase C modulates the insulin secretory process by maintaining a proper function of the beta-cell voltage-activated Ca2+ channels. J Biol Chem. 1994; 269(4):2743–9. PMID: 8300606

68. Wetzelberger K, Baba SP, Thirunavukkarasu M, Ho YS, Maulik N, Barski OA, et al. Postischemic deactivation of cardiac aldose reductase: role of glutathione S-transferase P and glutaredoxin in regeneration of reduced thiols from sulfenic acids. J Biol Chem. 2010; 285(34):26135–48. https://doi.org/10.1074/jbc.M110.146423 PMID: 20538586

69. Camaschella C, Campanella A, De Falco L, Boschetto L, Merlini R, Silvestri L, et al. The human counterpart of zebrafish shiraz shows sideroblastic-like microcytic anemia and iron overload. Blood. 2007; 110(4):1353–8. https://doi.org/10.1182/blood-2007-02-072520 PMID: 17485548

70. Dixon SJ, Stockwell BR. The role of iron and reactive oxygen species in cell death. Nat Chem Biol. 2014; 10(1):9–17. https://doi.org/10.1038/nchembio.1416 PMID: 24346035

71. Hansen JB, Tonnesen MF, Madsen AN, Hagedorn PH, Friberg J, Grunnet LG, et al. Divalent metal transporter 1 regulates iron-mediated ROS and pancreatic β cell fate in response to cytokines. Cell Metab. 2012; 16(4):449–61. https://doi.org/10.1016/j.cmet.2012.09.001 PMID: 23000401

72. Cooksey RC, Jones D, Gabrielsen S, Huang J, Simcox JA, Luo B, et al. Dietary iron restriction or iron chelation protects from diabetes and loss of beta-cell function in the obese (ob/ob lep-/-) mouse. Am J Physiol Endocrinol Metab. 2010; 298(6):E1236–43. https://doi.org/10.1152/ajpendo.00022.2010 PMID: 20354157